PHYSICAL REVIEW D **94,** 114501 (2016)

Fermion bag approach for the massive Thirring model at finite density

Daming Li*

School of Mathematical Sciences, Shanghai Jiao Tong University, Shanghai 200240, China

(Received 10 August 2016; published 2 December 2016)

We consider the $2+1$-dimensional massive Thirring model with one flavor at finite density. Two numerical methods, the fermion bag approach and complex Langevin dynamics, are used to calculate the chiral condensate and fermion density of this model. The numerical results obtained by the fermion bag approach are compared with those obtained by complex Langevin dynamics. They are also compared with those obtained under a phase-quenched approximation. We show that in some range of fermion coupling strength and chemical potential, the sign problem in the fermion bag approach is mild, while it becomes severe for the complex Langevin dynamics.

DOI: 10.1103/PhysRevD.94.114501

I. INTRODUCTION

The sign problem remains one of the biggest challenges in many fields, e.g., polymer field theory in condensed matter physics [1] and lattice field theory in high-energy physics. The usual sampling methods, e.g., Langevin dynamics and the Monte Carlo method, fail for the sign problem due to the high oscillation of complex action, where the Boltzmann factor cannot be regarded as the probability density. Because of the introduction of fields necessary to decouple repulsive interaction between monomers, the sign problem cannot be avoided for polymer field theory [2]. For the lattice field theory in high-energy physics, three reasons will always lead to the complex action: (1) grand partition function with finite density, (2) fermion systems, and (3) topological terms in the action.

To overcome the sign problem, the complex Langevin (CL) dynamics, which is obtained from the complexification of the Langevin dynamics, was used. The CL is rather successful in the XY model [3]; Bose gas [4]; the Thirring model [5]; Abelian and non-Abelian lattice gauge models [6]; the QCD model [7] and its simplified models, including the one link U(1) model, the one link SU(3) model, the QCD model in the heavy mass limit [8], the one link SU(N) model [9], the SU(3) spin model [10], and the Polyakov chain model [11]. It was also applied to quantum fields in nonequilibrium [12] and in real time [13,14]. For some range of chemical potential and large fluctuation, the complex Langevin may fail (e.g., the XY model at finite chemical potential for large fluctuation) [15] and in the Thirring model in $0+1$ dimension [16]. Unfortunately from early studies of complex Langevin evolutions [17–19] until this day, the convergence properties of complex Langevin equations are not well understood. Recently Aarts *et al.* provided a criterion for checking the correctness of the complex Langevin dynamics [20]. The recent discussion about complex Langevin dynamics can be found in Refs. [21–30].

Since the partition function is always real, it is possible to find suitable variables to represent this partition function with real action. This is called the dual variable method. It is successfully applied to many models, including Bose gas [31]; the SU(3) spin model [32]; U(1) and Z(3) gauge Higgs lattice theory [33]; the massive lattice Schwinger model [34]; the O(3), O(N), and CP(N-1) models [35–38]; the fermion bag approach [39]; 4-fermion lattice theory, including the massless Thirring model [40]; the Gross-Neveu model [41]; the Yukawa model [42]; the non-Abelian Yang-Mills model [43,44], and its coupling with fermion field [45]; the lattice chiral model; and the sigma model [46]. For the recent progress of solving the sign problem for nonrelativistic fermion systems, see Refs. [47–53].

For fermion systems, the dual method is called the fermion bag approach [39]. This numerical method overcomes the sign problem for models with small chemical potential, and also a high computational efficiency is achieved for the small or large interactions between fermions. We study the $2+1$-dimensional massive Thirring model at finite density (cf. [54]), which can be regarded as the effective theories of high-temperature superconductors and graphene; see, e.g., references given in [55]. We have studied this model at finite density in $0+1$ dimension and compared the complex Langevin dynamics and fermion bag approach [56]. In this paper we continue to compare the complex Langevin dynamics and the fermion bag approach for the massive Thirring model at finite density in $2+1$ dimensions.

The arrangement of the paper is as follows. In Sec. II, the fermion bag approach for the Thirring model is presented and the chiral condensate and fermion density are obtained. In Sec. III, the complex Langevin dynamics is given for this model by introducing the bosonic variable. In Sec. IV, the chiral condensate and fermion density are calculated by these two methods and are compared with each other. Conclusions are given in Sec. V.

*lidaming@sjtu.edu.cn

II. THIRRING MODEL

The lattice partition function for the massive Thirring model at the finite density in d-dimensional lattice $\Lambda = \{x = (x_0, \ldots, x_{d-1}), x_i = 0, \ldots, N-1, i = 0, \ldots, d-1\}$ with even N reads

$$Z = \int d\bar{\psi} d\psi e^{-S}, \tag{1}$$

where $d\bar{\psi}d\psi = \prod_{x\in\Lambda} d\bar{\psi}(x)d\psi(x)$ is the measure of the Grassmann fields $\psi = \{\psi(x)\}_{x\in\Lambda}$ and $\bar{\psi} = \{\bar{\psi}(x)\}_{x\in\Lambda}$. We adopt antiperiodic conditions for ψ and $\bar{\psi}$ in the x_0 direction and periodic conditions in the other directions,

$$\begin{aligned}&\psi(x + kN\hat{\alpha}) = (-1)^{k\delta_{\alpha,0}}\psi(x),\\ &\bar{\psi}(x + kN\hat{\alpha}) = (-1)^{k\delta_{\alpha,0}}\bar{\psi}(x), \quad x\in\Lambda, \quad k = 0, \quad \pm 1, \ldots,\end{aligned} \tag{2}$$

where $\hat{\alpha}$ denotes the unit vector in the α direction. The action S in (1) is

$$\begin{aligned}S = &\sum_{x,y\in\Lambda} \bar{\psi}(x) D_{x,y}\psi(y) - U\\ &\times \sum_{x\in\Lambda,\alpha=0,\ldots,d-1} \bar{\psi}(x)\psi(x)\bar{\psi}(x+\hat{\alpha})\psi(x+\hat{\alpha}),\end{aligned} \tag{3}$$

with non-negative coupling constant U between fermions. The fermion matrix D, which depends on the fermion mass m and chemical potential μ, is given by

$$\begin{aligned}D_{x,y} &= D(\mu, m)_{x,y}\\ &= \sum_{\alpha=0,\ldots,d-1} \frac{\eta_{x,\alpha}}{2}\left(e^{\mu\delta_{\alpha,0}} s^{+}_{x,\alpha}\delta_{x+\hat{\alpha},y} - e^{-\mu\delta_{\alpha,0}} s^{-}_{x,\alpha}\delta_{x,y+\hat{\alpha}}\right)\\ &\quad + m\delta_{x,y}\\ &= \begin{cases} \frac{\eta_{x,\alpha}}{2} e^{\mu\delta_{\alpha,0}} s^{+}_{x,\alpha} & \text{if } y = x+\hat{\alpha}\\ -\frac{\eta_{x,\alpha}}{2} e^{-\mu\delta_{\alpha,0}} s^{-}_{x,\alpha} & \text{if } y = x-\hat{\alpha}\\ m & \text{if } y = x\\ 0 & \text{otherwise}\end{cases},\end{aligned} \tag{4}$$

with staggered phase factors $\eta_{x,0} = 1$, $\eta_{x,\alpha} = (-1)^{x_0+\cdots+x_{\alpha-1}}$, $\alpha = 1, \ldots, d-1$, satisfying $\eta_{x+\hat{\alpha},\alpha} = \eta_{x,\alpha}$. The boundary condition for ψ and $\bar{\psi}$ are accounted for by the sign functions s^{+} and s^{-},

$$\begin{aligned}s^{+}_{x,\alpha} &= \begin{cases} -1 & \text{if } \alpha = 0 \quad \text{and} \quad x_0 = N-1\\ 1 & \text{otherwise}\end{cases},\\ s^{-}_{x,\alpha} &= \begin{cases} -1 & \text{if } \alpha = 0 \quad \text{and} \quad x_0 = 0\\ 1 & \text{otherwise}\end{cases},\end{aligned} \tag{5}$$

with periodic extensions for s^{+} and s^{-} with respect to x for any direction α. These two sign functions satisfy $s^{+}_{x,\alpha} = s^{-}_{x+\hat{\alpha},\alpha}$ for any lattice x and any direction α.

The fermion matrix has two kind of symmetries with respect to μ and m, which leads to the symmetry of the determinant $\det D$ (note that N is even),

$$\begin{aligned}D(\mu, m)_{x,y} &= -D(-\mu, -m)_{y,x} \Rightarrow \det D(\mu, m)\\ &= \det D(-\mu, -m)\end{aligned} \tag{6}$$

$$\begin{aligned}\varepsilon_x D(\mu, m)_{x,y}\varepsilon_y &= -D(\mu, -m)_{x,y} \Rightarrow \det D(\mu, m)\\ &= \det D(\mu, -m),\end{aligned} \tag{7}$$

where $\varepsilon_x = (-1)^{x_0+\cdots+x_{d-1}}$ is the parity of site x. Thus it is sufficient to study the massive Thirring model for $\mu \geq 0$ and $m \geq 0$.

The fermion bag approach for the Thirring model is based on the high-temperature expansion of the interacting term:

$$\begin{aligned}&\exp\left(U \sum_{x\in\Lambda,\alpha=0,\ldots,d-1} \bar{\psi}(x)\psi(x)\bar{\psi}(x+\hat{\alpha})\psi(x+\hat{\alpha})\right)\\ &= \prod_{x\in\Lambda,\alpha=0,\ldots,d-1} \sum_{k_{x,\alpha}=0}^{1} \left(U\bar{\psi}(x)\psi(x)\bar{\psi}(x+\hat{\alpha})\psi(x+\hat{\alpha})\right)^{k_{x,\alpha}}.\end{aligned} \tag{8}$$

Inserting this expansion into the partition function in (1), one has an expansion of Z with respect to U,

$$Z = \sum_{k=(k_{x,\alpha})} U^j C(x_1, \ldots, x_{2j}), \tag{9}$$

where the summation is taken over all configurations k with $k_{x,\alpha} = 0, 1$ for both neighboring sites $(x, x+\hat{\alpha})$ and $\sum_{\alpha=0}^{d-1} k_{x,\alpha}$ must be 0 or 1 for all sites x. If $k_{x,\alpha} = 1$, we say there is a bond connecting x and $x+\hat{\alpha}$; otherwise, there are no bonds connecting them. For a given configuration k, for example, there are j bonds $(x_1, x_2), \ldots, (x_{2j-1}, x_{2j})$ connecting $2j$ different sites, and the weight in (9) depending on these $2j$ different sites $\{x_i\}_{i=1}^{2j}$ is

$$\begin{aligned}C(x_1, \ldots, x_{2j}) &= \int d\bar{\psi}d\psi \exp\left(-\sum_{x,y} \bar{\psi}(x) D_{x,y}\psi(y)\right)\\ &\quad \times \bar{\psi}(x_1)\psi(x_1)\cdots\bar{\psi}(x_{2j})\psi(x_{2j})\\ &= \det D \det G(\{x_1, \ldots, x_{2j}\})\\ &= \det D(\backslash\{x_1, \ldots, x_{2j}\}),\end{aligned} \tag{10}$$

where $G(\{x_1, \ldots, x_{2j}\})$ is a $(2j)\times(2j)$ matrix of propagators between $2j$ sites x_i, $i = 1, \ldots, 2j$, whose matrix elements are $G(\{x_1, \ldots, x_{2j}\})_{i,l} = D^{-1}_{x_i,x_l}$, $i, l = 1, \ldots, 2j$.

The matrix $G(\{x_1,\ldots,x_{2j}\})$ depends on the order of $\{x_1,\ldots,x_{2j}\}$, but its determinant does not. $D(\backslash\{x_1,\ldots,x_{2j}\})$ is the $(N^d-2j)\times(N^d-2j)$ matrix that is obtained by deleting rows and columns corresponding to sites $x_1,\ldots,x_{2j}$. The first equality in (10) holds due to the basic Gaussian integration for the Grassmann variables [57]. In the second equality of (10), we expand the exponential and then integrate the Grassmann variables $\{x_i\}_{i=1}^{2j}$. The average number of bonds depends on the interaction strength U between fermions. If U is small, there are few bonds between two neighboring sites, and we use $G(\{x_1,\ldots,x_{2j}\})$ to calculate $C(x_1,\ldots,x_{2j})$; otherwise, U is large and there are many occupied bonds between neighboring sites, and thus $D(\backslash\{x_1,\ldots,x_{2j}\})$ is used to calculate $C(x_1,\ldots,x_{2j})$. For any number of different sites $\{x_i\}_{i=1}^{n}$, the function $C=C(x_1,\ldots,x_n;D(\mu,m))$ depends on the fermion matrix $D(\mu,m)$.

Because of the symmetry (6) and (7) of D, the function C for any different site $\{x_i\}_{i=1}^{n}$ has the symmetry (see Appendix A)

$$\begin{aligned}C(x_1,\ldots,x_n;D(\mu,m)) &= (-1)^n C(x_1,\ldots,x_n;D(\mu,-m))\\ &= C(x_1,\ldots,x_n;D(-\mu,m))\\ &= (-1)^n C(x_1,\ldots,x_n;D(-\mu,-m))\end{aligned} \tag{11}$$

for any real number μ and m. According to the representation of the partition function in (9), where $n=2j$ is even, the weight C becomes nonnegative for any μ and m if $C(x_1,\ldots,x_n;D(\mu,m))$ is nonnegative for any even number of sites $(x_1,\ldots,x_n)$ and for any nonnegative μ and nonnegative m. Unfortunately C is not always positive and thus the sign problem still exist. But we want to justify that the sign problem in the representation of (9) is rather mild.

If $d=1$, we can prove that for any $\mu>0$ and $m>0$, $C(x_1,\ldots,x_n;D(\mu,m))>0$ for any number of different sites $\{x_i\}_{i=1}^{n}$ (see Appendix B). If $\mu=0$ and $m=0$, the fermion matrix D is real and anti-Hermitian and thus its eigenvalues come in complex conjugate pairs with vanishing real parts. If $\mu=0$ and $m>0$, the determinant of D is positive. $D(\backslash\{x_1,\ldots,x_{2j}\})$ ($\mu=0$ and $m=0$) is also real and anti-Hermitian since the rows and columns corresponding to these sites are deleted. Thus if $\mu=0$ and $m>0$, $C(x_1,\ldots,x_n;D(\mu,m))>0$ for any configuration k and any dimension d. The numerical test shows that the function C in (10) for $d>1$ is always positive for any configuration k if $\mu\geq 0$ is close to zero. When μ is increased, C may be negative for some configurations. The left panel of Fig. 1 shows that the frequency of negative C for a two-dimensional Thirring model is rather small, which is less than 0.1. For the three-dimensional Thirring model, the frequency of negative C becomes larger (close to 0.35 when $\mu=2$). Moreover, when μ is increased, the frequency of negative C also becomes larger. In fact, our simulation shows that this frequency is zero when $\mu\leq 1.3$ for both two- and three-dimensional Thirring models. Thus the presentation of the partition function (9) avoids the sign problem at least for small chemical potential.

The chiral condensate is

$$\langle\bar{\psi}\psi\rangle=\frac{1}{N^d}\frac{\partial\ln Z}{\partial m}=\frac{1}{N^d}\left\langle\frac{\partial_m C(x_1,\ldots,x_{2j})}{C(x_1,\ldots,x_{2j})}\right\rangle, \tag{12}$$

where the average is taken with respect to the weight of the partition function (9). Similar to the calculation of C in (10), the ratio $\partial_m C/C$ has two formulas:

$$\begin{aligned}\frac{\partial_m C(x_1,\ldots,x_{2j})}{C(x_1,\ldots,x_{2j})} &= \sum_{x\neq x_1,\ldots,x_{2j}}\frac{\det G(\{x,x_1,\ldots,x_{2j}\})}{\det G(\{x_1,\ldots,x_{2j}\})}\\ &= \sum_{x\neq x_1,\ldots,x_{2j}}\frac{\det D(\backslash\{x,x_1,\ldots,x_{2j}\})}{\det D(\backslash\{x_1,\ldots,x_{2j}\})}.\end{aligned} \tag{13}$$

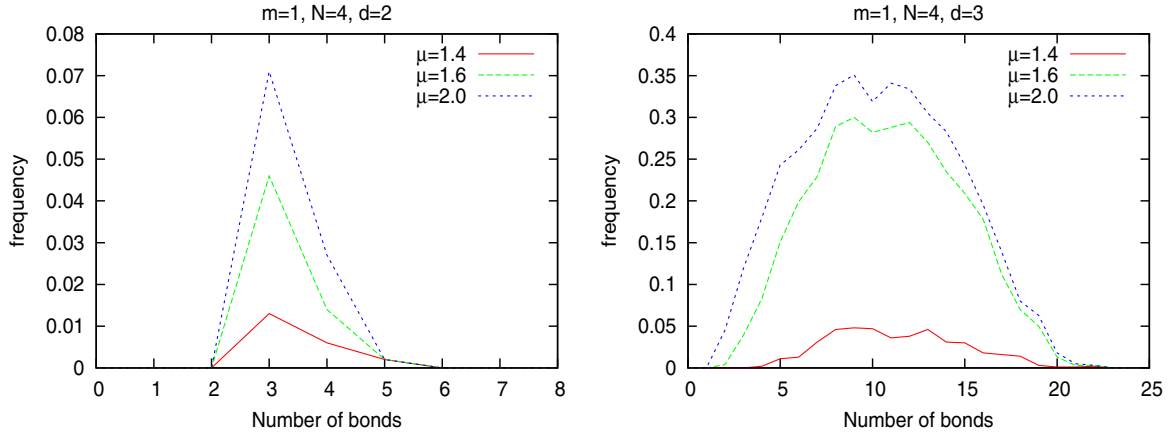

FIG. 1. Frequency of negative C where the configurations $k=(k_{x,\alpha})$ are chosen randomly.

The ratio between the determinants of submatrix G can be obtained by

$$\frac{\det G(\{x,x_1,\ldots,x_{2j}\})}{\det G(\{x_1,\ldots,x_{2j}\})} = G(\{x\}) - G(x,\text{occu\_sites})G(\{x_1,\ldots,x_{2j}\})^{-1} \times G(\text{occu\_sites},x), \quad (14)$$

where occu_sites $=(x_1,\ldots,x_{2j})$ denotes $2j$ occupied sites and $G(x,\text{occu\_sites})$ is a row vector with $2j$ components, D^{-1}_{x,x_i}, $i=1,\ldots,2j$. The column vector $G(\text{occu\_sites},x)$ is the transpose of $G(x,\text{occu\_sites})$. The ratio between the determinant of submatrix D is

$$\frac{\det D(\backslash\{x,x_1,\ldots,x_{2j}\})}{\det D(\backslash\{x_1,\ldots,x_{2j}\})} = \text{D\_Inv}(x,x), \quad (15)$$

where $\text{D\_Inv}(x,x)$ is the diagonal element of $D(\backslash\{x_1,\ldots,x_{2j}\})^{-1}$ corresponding to the site $x\neq x_1,\ldots,x_{2j}$.

Similarly, the fermion density,

$$\langle n\rangle = \frac{1}{N^d}\frac{\partial \ln Z}{\partial\mu} = \frac{1}{N^d}\left\langle \frac{\partial_\mu C(x_1,\ldots,x_{2j})}{C(x_1,\ldots,x_{2j})}\right\rangle, \quad (16)$$

can also be calculated.

The Monte Carlo algorithm based on the partition function in (9) can be found in Ref. [40]. We adopt the following three steps to update the current configuration. Assume that the current configuration k has n_b bonds:

$$C=([x_1,x_2],\ldots,[x_{2n_b-1},x_{2n_b}]).$$

Try to delete a bond, e.g., $[x_{2n_b-1},x_{2n_b}]$, from the current configuration C to be

$$C'=([x_1,x_2],\ldots,[x_{2n_b-3},x_{2n_b-2}]).$$

According to the detailed balance,

$$W(C)P_{\text{try}}(C\to C')P_{\text{acc}}(C\to C') = W(C')P_{\text{try}}(C'\to C)P_{\text{acc}}(C'\to C), \quad (17)$$

where $W(C)$ and $W(C')$ are the weights in the partition function (9) for the configurations C and C', respectively. The try probabilities from $C(C')$ to $C'(C)$ are

$$P_{\text{try}}(C\to C')=\frac{1}{n_b},\qquad P_{\text{try}}(C'\to C)=\frac{1}{n_f},$$

respectively. Here n_f is the number of bonds that can be created from the configuration C'. Thus the accept probability from C to C' is

$$P_{\text{acc}}(C\to C')=\frac{n_b}{n_f}\frac{W(C')}{W(C)}.$$

Try to add a bond, e.g., $[x_{2n_b+1},x_{2n_b+2}]$, from the current configuration C to be

$$C'=([x_1,x_2],\ldots,[x_{2n_b-1},x_{2n_b}],[x_{2n_b+1},x_{2n_b+2}]).$$

The detailed balance is Eq. (17), where

$$P_{\text{try}}(C\to C')=\frac{1}{n_f},\qquad P_{\text{try}}(C'\to C)=\frac{1}{n_b+1}.$$

Here n_f is the number of bonds that can be created from the configuration C. Thus the accept probability from C to C' is

$$P_{\text{acc}}(C\to C')=\frac{n_f}{n_b+1}\frac{W(C')}{W(C)}.$$

Try to delete a bond, e.g., $[x_{2n_b-1},x_{2n_b}]$, from the current configuration C and then add a bond, e.g., $[y_{2n_b-1},y_{2n_b}]$,

$$C'=([x_1,x_2],\ldots,[x_{2n_b-3},x_{2n_b-2}],[y_{2n_b-1},y_{2n_b}]).$$

In the detailed balance (17),

$$P_{\text{try}}(C\to C')=P_{\text{try}}(C'\to C)=\frac{1}{n_bn_f}.$$

Here n_f is the number of bonds that can be created from the configuration C, where $[x_{2n_b-1},x_{2n_b}]$ is deleted. Thus the accept probability to move a bond is

$$P_{\text{acc}}(C\to C')=\frac{W(C')}{W(C)}.$$

III. COMPLEX LANGEVIN DYNAMICS

The expansion of (8) can also be written as an integral of bosonic variables $A_\alpha(x)$ by Hubbard-Stratonovich transformation,

$$\exp\left(U\sum_{x,\alpha=0,\ldots,d-1}\bar\psi(x)\psi(x)\bar\psi(x+\hat\alpha)\psi(x+\hat\alpha)\right) = \prod_{x,\alpha}\left(\frac{1}{2\pi U}\right)^{1/2}\int\prod_{x,\alpha}dA_\alpha(x)\exp\left(-\frac{1}{8U}\sum_{x,\alpha}A^2_\alpha(x)\right) \times\exp\left(-\sum_{x,y}\bar\psi(x)\sum_\alpha i\frac{1}{2}(B_{x,\alpha}A_\alpha(x)\delta_{x+\hat\alpha,y} + C_{x-\hat\alpha,\alpha}A_\alpha(y)\delta_{x,y+\hat\alpha})\psi(y)\right), \quad (18)$$

for any two bosonic fields $B_{x,\alpha}$ and $C_{x,\alpha}$, satisfying $B_{x,\alpha}C_{x,\alpha}=1$.

Choosing

$$B_{x,\alpha}=e^{\mu\delta_{\alpha,0}}\eta_{x,\alpha},\qquad C_{x,\alpha}=e^{-\mu\delta_{\alpha,0}}\eta_{x,\alpha},\tag{19}$$

inserting (18) into the partition function Z in (1), and integrating the Grassmann fields ψ, $\bar{\psi}$, we have

$$\begin{aligned}Z&=\int\prod_{x,\alpha}dA_\alpha(x)\exp\left(-\frac{1}{8U}\sum_{x,\alpha}A_\alpha^2(x)\right)\det K\\&=\int\prod_{x,\alpha}dA_\alpha(x)e^{-S_{\rm eff}},\end{aligned}\tag{20}$$

where we omitted the factor $\prod_{x,\alpha}(\frac{1}{2\pi U})^{1/2}$. The matrix K depends on A,

$$\begin{aligned}K_{x,y}=&\sum_{\alpha=0,\ldots,d-1}\frac{\eta_{x,\alpha}}{2}((s^+_{x,\alpha}+iA_\alpha(x))e^{\mu\delta_{\alpha,0}}\delta_{x+\hat{\alpha},y}\\&-(s^-_{x,\alpha}-iA_\alpha(y))e^{-\mu\delta_{\alpha,0}}\delta_{x,y+\hat{\alpha}})+m\delta_{x,y},\end{aligned}\tag{21}$$

which is complex, although the field A is real. The matrix K is reduced to be D in (4) if A_α vanishes. The effective action in (20) is

$$S_{\rm eff}=\frac{1}{8U}\sum_{x,\alpha}A_\alpha^2(x)-\ln\det K.\tag{22}$$

The complex Langevin dynamics reads

$$\begin{aligned}A_\alpha(x,\Theta+\Delta\Theta)=&A_\alpha(x,\Theta)-\Delta t\frac{\partial S_{\rm eff}}{\partial A_\alpha(x,\Theta)}\\&+\sqrt{2\Delta t}\eta_\alpha(x,\Theta),\end{aligned}\tag{23}$$

where Θ denotes the discrete complex Langevin time and $\Delta\Theta$ is the time step. The real white noise $\eta_{x,\Theta}$ satisfies

$$\langle\eta_\alpha(x,\Theta)\eta_{\alpha'}(x',\Theta')\rangle=\delta_{\alpha,\alpha'}\delta_{x,x'}\delta_{\Theta,\Theta'}.$$

The drift force can be written as

$$\begin{aligned}-\frac{\partial S_{\rm eff}}{\partial A_\alpha(x)}&=-\frac{1}{4U}A_\alpha(x)+{\rm Tr}\left(K^{-1}\frac{\partial K}{\partial A_\alpha(x)}\right)\\&=-\frac{1}{4U}A_\alpha(x)+\frac{i}{2}(\eta_{x,\alpha}e^{\mu\delta_{\alpha,0}}K^{-1}_{x+\hat{\alpha},x}\\&\quad+\eta_{x+\hat{\alpha},\alpha}e^{-\mu\delta_{\alpha,0}}K^{-1}_{x,x+\hat{\alpha}}).\end{aligned}\tag{24}$$

The chiral condensate in (12) is written as

$$\langle\bar{\psi}\psi\rangle=\frac{1}{N^d}\langle{\rm Tr}(K^{-1})\rangle\tag{25}$$

and the fermion density in (16) reads

$$\langle n\rangle=\frac{1}{N^d}\left\langle{\rm Tr}\left(K^{-1}\frac{\partial K}{\partial\mu}\right)\right\rangle,\tag{26}$$

where the average is taken with respect to weight $e^{-S_{\rm eff}}$. Note that

$$\begin{aligned}{\rm Tr}\left(K^{-1}\frac{\partial K}{\partial\mu}\right)=&\sum_{x,y}K^{-1}_{y,x}\left(\frac{e^\mu}{2}(s^+_{x,0}+iA_0(x))\delta_{x+\hat{0},y}\right.\\&\left.+\frac{e^{-\mu}}{2}(s^-_{x,0}-iA_0(y))\delta_{x,y+\hat{0}}\right).\end{aligned}$$

If we can choose instead of (19)

$$B_{x,\alpha}=e^{\mu\delta_{\alpha,0}}\eta_{x,\alpha}s^+_{x,\alpha},\qquad C_{x,\alpha}=e^{-\mu\delta_{\alpha,0}}\eta_{x,\alpha}s^-_{x+\hat{\alpha},\alpha},$$

satisfying $B_{x,\alpha}C_{x,\alpha}=1$, the partition function Z can also be written as Eq. (20), where the matrix K is replaced by

$$\begin{aligned}\tilde{K}_{x,y}=&\sum_{\alpha=0,\ldots,d-1}\frac{\eta_{x,\alpha}}{2}(s^+_{x,\alpha}(1+iA_\alpha(x))e^{\mu\delta_{\alpha,0}}\delta_{x+\hat{\alpha},y}\\&-s^-_{x,\alpha}(1-iA_\alpha(y))e^{-\mu\delta_{\alpha,0}}\delta_{x,y+\hat{\alpha}})+m\delta_{x,y}.\end{aligned}\tag{27}$$

IV. SIMULATION RESULTS

The implementation of the fermion bag approach and complex Langevin dynamics can be found in [56]. We use the Γ method to estimate the error for the samples in each Monte Carlo simulation or complex Langevin dynamics [58]. The following simulation results are given for one- and three-dimensional Thirring model with fixed $N=8$, $m=1$ but with different coupling strength U and different chemical potential $0\le\mu\le 2$.

Figures 2 and 3 show the comparison of the chiral condensate and fermion density obtained by the fermion bag approach (FB) and by complex Langevin dynamics for different chemical potential μ and coupling strength U. Both these averages agree with each other very well by these two numerical methods. The statistic errors are almost invisible in Figs. 2 and 3. When the coupling strength U is increasing, e.g., $U=0.25$, the chiral condensate and fermion density obtained by FB and by CL are quite different for the intermediate values of chemical potential μ, as shown in Fig. 4. One reason for this difference is related to the severeness of the sign problem, which can be measured by the phase $\langle e^{i\varphi}\rangle_{\rm pq}=Z/Z_{\rm pq}$. The sign problem is rather severe for CL, while it is still mild for FB if $1\le\mu\le 2$. We thus compare the results obtained by these two numerical methods under the phase-quenched approximation (see Appendix D). The chiral condensate and fermion density agree with each other for FB and this method under phase-quenched approximation [FB(pq)]. However, these agreements cannot be achieved for CL

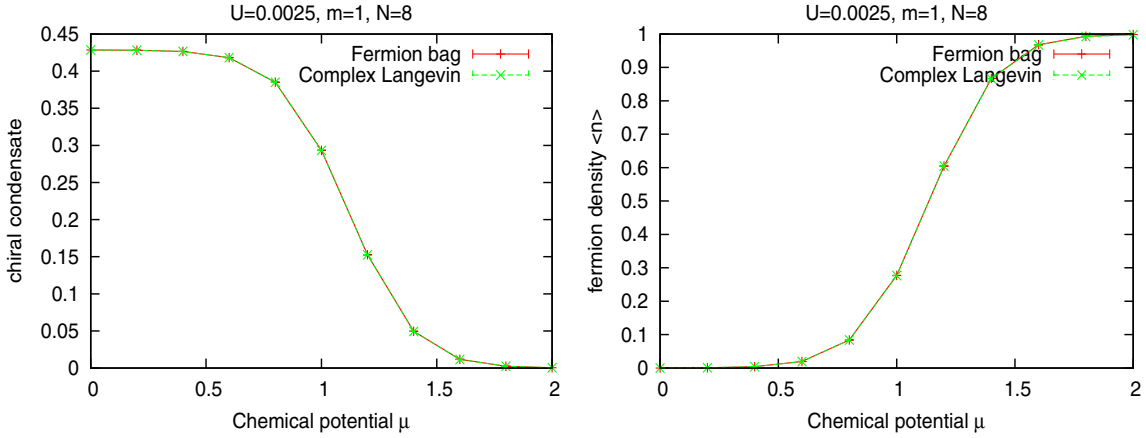

FIG. 2. Comparison of the chiral condensate and fermion density obtained by complex Langevin dynamics and by the fermion bag approach. In the fermion bag approach, the sampling starts after 1×10^6 Monte Carlo steps and ends after 1×10^7 steps. Two sequential samples are separated by $10 \times 3 \times N^3$ Monte Carlo steps. In complex Langevin dynamics, $\Delta\Theta = 0.001$, the equilibrium Langevin time $t_{\rm eq} = 20$ and the sampling end time $t_{\rm end} = 40$. Two sequential samples are separated by 10 complex Langevin steps.

and the complex Langevin dynamics under phase-quenched approximation [CL(pq)]. The severity of the sign problem by both approaches is shown in Fig. 5. Because the determinant $\det(K)$ of K becomes too large if $\mu > 1.6$, we just calculate the phase $\langle e^{i\varphi}\rangle_{\rm pq}$ by CL for $0 \le \mu \le 1.6$. We also calculate this phase by FB for different U values and different chemical potential $0 \le \mu \le 2$. For $U = 0.25$, the phase $\langle e^{i\varphi}\rangle_{\rm pq}$ is almost very close to 1 for FB in $0 \le \mu \le 2$. Thus the sign problem is almost overcome and this can explain why the results obtained by FB agree with those obtained under the quenched approximation [FB(pq); see Fig. 4]. The sign problem for FB becomes severe during the intermediate range of the chemical potential, as shown for $U = 0.25$, 1.0, 2.0. Moreover this range shifts to larger chemical potential if U is increased. For CL with $U = 0.25$, the phase drops very fast to zero if $\mu > 0.6$ and is very close to zero for $\mu \ge 1$. This also explains the difference between those obtained by CL and by CL(pq) in Fig. 4.

As shown in Fig. 5, the (real part of) the phase drops rapidly in the intermediate value of μ ($0.6 \le \mu \le 1.2$) for CL [$U = 0.25$(CL)]. Although the statistical error of the chiral condensate and fermion density in this range of μ is larger than those for $\mu < 0.6$ or $\mu > 1.2$, the statistical error in the whole range of μ ($0 \le \mu \le 2$) is almost invisible in Fig. 4. In Fig. 6, we compared the chiral condensate obtained by FB and by CL with the exact result for a one-dimensional Thirring model with the same parameters [56]. The chiral condensate obtained by FB agrees with the exact result in the whole range of μ, while the chiral condensate by CL is slightly smaller than the exact result in the intermediate value of μ, where the phase $Z/Z_{\rm pq}$ drops rapidly from 1 to 0 for CL. These results are quite similar to those in the left panel of Fig. 4, where the

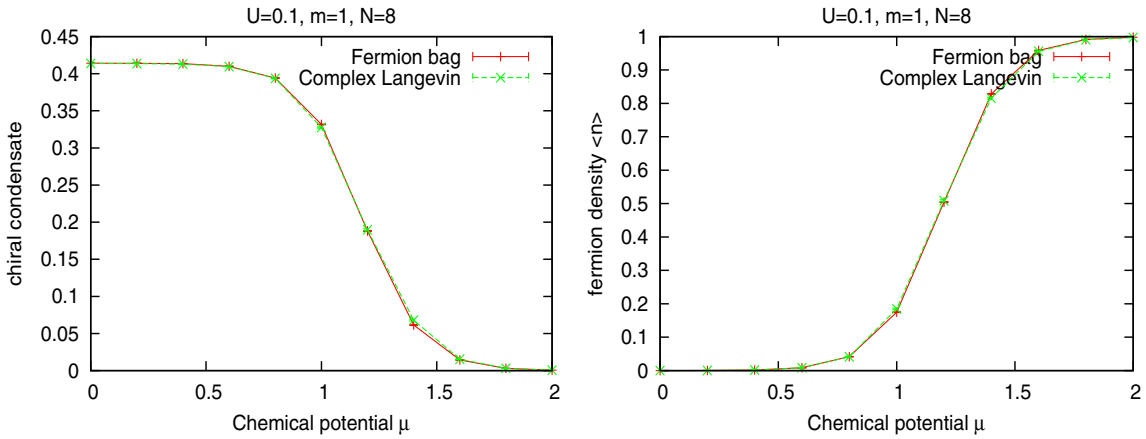

FIG. 3. Parameters are the same as those in Fig. 2, except U.

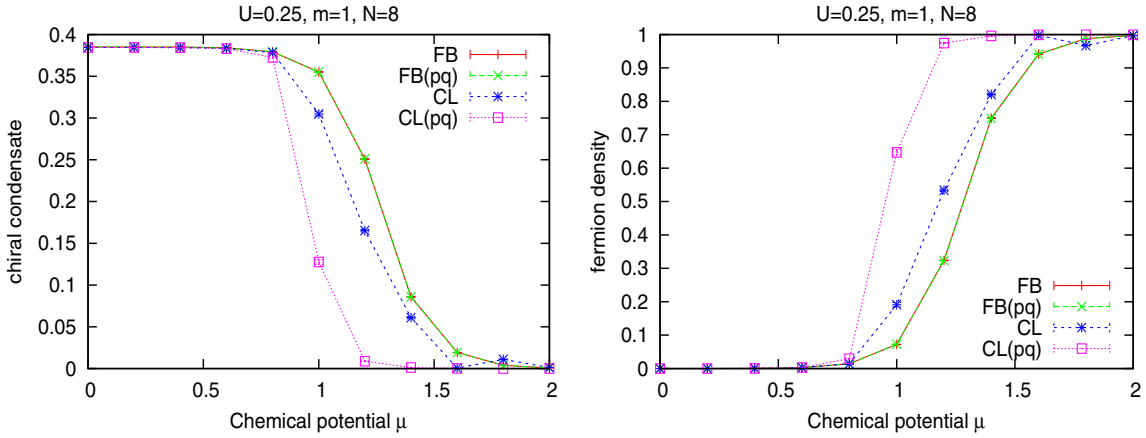

FIG. 4. Parameters are the same as those in Fig. 2, except U, for FB and CL, with phase-quenched approximations (pq).

chiral condensate obtained by CL is smaller than those obtained by FB for the intermediate value of μ. The statistical error for CL in the left panel of Fig. 4 is smaller than those in Fig. 6.

Our calculation for the chiral condensate and fermion density in one- and three-dimensional Thirring models at finite density by CL quantitatively agrees with those obtained by Pawlowski and Zielinski [5,16]. Compared with the lower panel of Fig. 3 in Ref. [5], where $\beta = 1 = 1/(4U)$, i.e., $U = 0.25$, our result by CL is closer to those obtained by FB in the left panel of Fig. 4. When $\mu = 1$, the chiral condensates are 0.305 ± 0.0027 by CL and 0.356 ± 0.00011 by FB, respectively, in the left panel of Fig. 4 while it is 0.25 in the lower panel of Fig. 3 in Ref. [5]. The statistical error is also almost invisible in Fig. 3 of Ref. [5] in the intermediate value of μ, where the phase drops rapidly in this range as shown in Fig. 4 of Ref. [5]. We can also compare the chiral condensate of the one-dimensional Thirring model in Fig. 6 with Fig. 5(b) in Ref. [16]. Our result in Fig. 6 by CL is better than those in Fig. 5(b) of [16]. For example, at $\mu = 1$, the chiral condensate obtained by CL is 0.27 ± 0.03 and the exact value is 0.293 in Fig. 6, while it is 0.14 ± 0.023 in Fig. 5 (b) in Ref. [16]. Moreover, the statistical errors in Fig. 5(b) of Ref. [16] are larger than those (e.g., Fig. 3 in Ref. [5]) in the three-dimensional Thirring model at finite density, which are quite similar to the statistical error in our calculation by CL for one- and three-dimensional Thirring model.

The discussion above shows that the difference in chiral condensates obtained by CL and by FB in the intermediate value of μ is definitely related to the fast decay of the real part of phase $\langle e^{i\varphi} \rangle_{\rm pq}$, i.e., the severity of the sign problem, although the statistical error is small as shown in Fig. 4. According to Refs. [16,20], the quantity

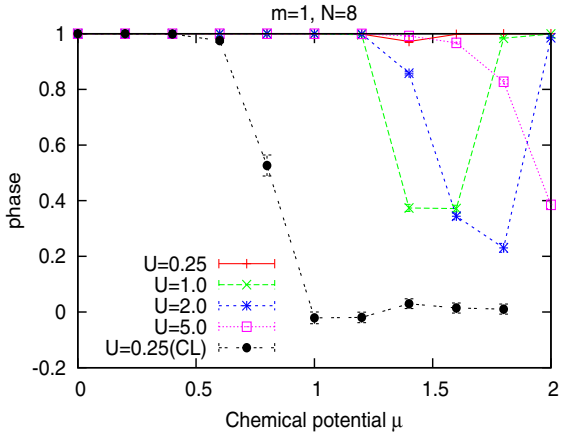

FIG. 5. The real part of phase $\langle e^{i\varphi} \rangle_{\rm pq}$ obtained by the fermion bag approach for $U = 0.25$, 1.0, 2.0, 5.0 and by complex Langevin dynamics for $U = 0.25$ [$U = 0.25$(CL)].

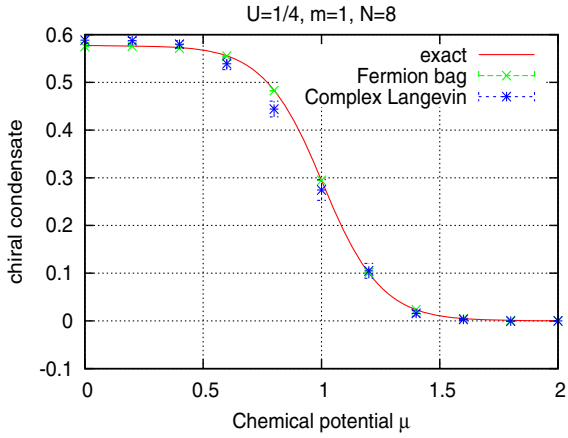

FIG. 6. Comparison among the fermion bag approach, complex Langevin dynamics, and the exact solution for the one-dimensional Thirring model (see Ref. [56]).

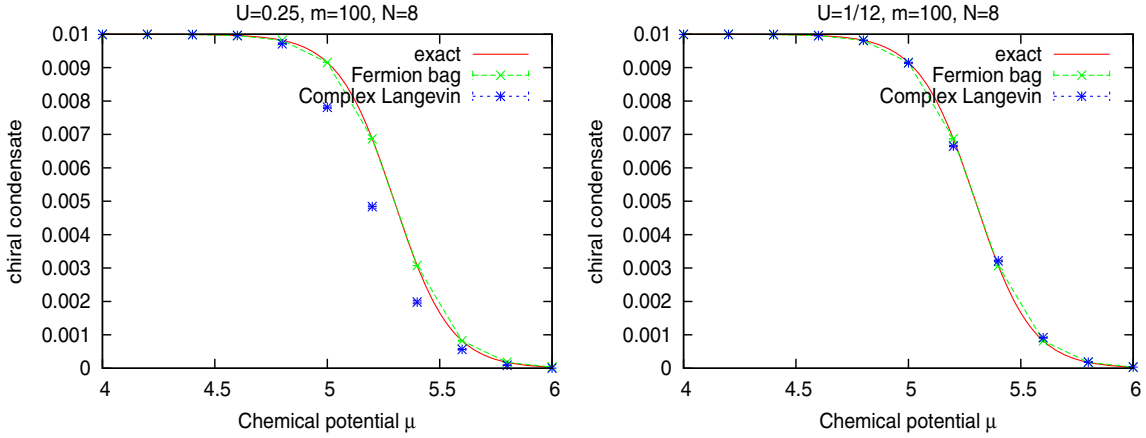

FIG. 7. The chiral condensate in the heavy quark limit for coupling strength $U = 0.25$ (left) and $U = 1/12 = 0.08333$ (right). Parameters are the same as those in Fig. 2, except U and m.

$$\langle \mathrm{LO} \rangle \equiv \left\langle \sum_{x,\mu} \left(\frac{d}{dA_\mu(x)} - \frac{dS_{\mathrm{eff}}}{dA_\mu(x)} \right) \frac{d}{dA_\mu(x)} O(A) \right\rangle \tag{28}$$

should vanish for any holomorphic function $O(A)$ if CL works. We choose the observable (the chiral condensate) $O(A) = \frac{1}{N^d}\mathrm{Tr}(K^{-1})$ for $\mu = 1$, $m = 1$, and $N = 8$. In the one-dimensional case, $\langle \mathrm{LO} \rangle$ is 0.0137 ± 0.00708 if $U = 0.0025$ and becomes -5.88 ± 7.33 if $U = 0.16$. In the three-dimensional case, $\langle \mathrm{LO} \rangle$ is -1.207 ± 0.0025 if $U = 0.0025$, 61.6 ± 64.02 if $U = 0.1$, and -206.3 ± 420.7 if $U = 0.25$. Thus $\langle \mathrm{LO} \rangle$ becomes large if U is increased and the chiral condensate by CL for $\mu = 1$ in the left panel of Fig. 4 is not reliable.

Finally we also compare the chiral condensate obtained by FB and by CL for the one-dimensional Thirring model with parameters $U = 10$, $m = 1$, and $N = 8$ (Fig. 5 in [56]). FB recovers the exact result for large coupling strength $U = 10$ for the chemical potential $0 \le \mu \le 2$, while the result obtained by CL is totally wrong. This is because there is no sign problem in FB in the one-dimensional Thirring model, while the sign problem is very severe in CL.

In the heavy fermion limit

$$m \to \infty, \qquad \mu \to \infty, \qquad \zeta \equiv (2m)^{-1} e^{\mu} \quad \text{fixed},$$

the exact solution is known [5], which does not depend on U (see Appendix C). Figure 7 shows the comparison between the condensate calculated by FB and by CL with the exact solution for different coupling strengths U in this limit. The results obtained by FB agree with the exact result for the different coupling strengths U. The results obtained by CL agree with the exact result only when U is small, e.g., $U = 1/12$. When U is increased, e.g., $U = 0.25$, the chiral condensate obtained by CL is less than the exact result in the intermediate range of chemical potential $4.8 \le \mu \le 5.6$, which was also found in Ref. [5].

V. CONCLUSIONS

The three-dimensional massive Thirring model at finite density is solved by two numerical methods: the fermion bag approach and complex Langevin dynamics. Two average quantities, chiral condensate and fermion density, are calculated and compared by these numerical methods. If the fermion coupling strength U is small, these averages obtained by the fermion bag approach agree with those obtained by complex Langevin dynamics. When U and the chemical potential are increasing, the sign problem for complex Langevin becomes severe; the results obtained by complex Langevin dynamics are quite different from those obtained under the phase-quenched approximation. For the parameters, the sign problem becomes severe for complex Langevin dynamics, but the sign problem for the fermion bag approach is still mild, and thus the results obtained by the fermion bag approach are reliable for these model parameters. Moreover, in the heavy quark limit, the fermion bag approach can recover the exact result for large coupling strength U, while the complex Langevin dynamics just recover the exact result for small coupling strength U. I believe that these advantages of the fermion bag approach over complex Langevin dynamics can be checked for the other interacting fermion systems with finite density, e.g., the Gross-Neveu model, Yukawa model, etc.

ACKNOWLEDGMENTS

I would like to thank Professor Shailesh Chandrasekharan for discussion. Daming Li was supported by the National Science Foundation of China (Grants No. 11271258 and No. 11571234).

APPENDIX A: PROOF OF (11)

For any different sites $\{x_i\}_{i=1}^n$,

$$\begin{aligned}
C(x_1,\ldots,x_n;D(\mu,m)) &= \int d\bar\psi d\psi \exp\left(-\sum_{x,y}\bar\psi(x)D(\mu,m)_{x,y}\psi(y)\right)\bar\psi(x_1)\psi(x_1)\cdots\bar\psi(x_n)\psi(x_n)\\
&= \int d\bar\chi d\chi \exp\left(-\sum_{x,y}\chi(x)D(\mu,m)_{x,y}\bar\chi(y)\right)\chi(x_1)\bar\chi(x_1)\cdots\chi(x_n)\bar\chi(x_n), \qquad \bar\psi\to\chi, \qquad \psi\to\bar\chi\\
&= \int d\bar\chi d\chi \exp\left(\sum_{x,y}\chi(x)D(-\mu,-m)_{y,x}\bar\chi(y)\right)\chi(x_1)\bar\chi(x_1)\cdots\chi(x_n)\bar\chi(x_n) \quad \text{by (6)}\\
&= (-1)^n\int d\bar\chi d\chi \exp\left(-\sum_{x,y}\bar\chi(x)D(-\mu,-m)_{x,y}\chi(y)\right)\bar\chi(x_1)\chi(x_1)\cdots\bar\chi(x_n)\chi(x_n)\\
&= (-1)^n C(x_1,\ldots,x_n;D(-\mu,-m)). \qquad \text{(A1)}
\end{aligned}$$

In the second equality we used $d\bar\psi d\psi = d\chi d\bar\chi = d\bar\chi d\chi$, since there is an even number of sites. By the symmetry (7) of D,

$$\begin{aligned}
C(x_1,\ldots,x_n;D(\mu,m)) &= \int d\bar\psi d\psi \exp\left(\sum_{x,y}\bar\psi(x)\varepsilon_x D(\mu,-m)_{x,y}\varepsilon_y\psi(y)\right)\bar\psi(x_1)\psi(x_1)\cdots\bar\psi(x_n)\psi(x_n)\\
&= (-1)^n\int d\bar\chi d\chi \exp\left(-\sum_{x,y}\bar\chi(x)D(\mu,-m)_{x,y}\chi(y)\right)\bar\chi(x_1)\chi(x_1)\cdots\bar\chi(x_n)\chi(x_n)\\
&= (-1)^n C(x_1,\ldots,x_n;D(\mu,-m)), \qquad \text{(A2)}
\end{aligned}$$

where in the second equality we used $\bar\psi(x) = -\varepsilon_x\bar\chi(x)$, $\psi(x) = \varepsilon_x\chi(x)$, and thus $d\bar\psi d\psi = d\bar\chi d\chi$ due to an even number of sites. Combing (A1) and (A2), we obtain (11).

APPENDIX B: THERE IS NO SIGN PROBLEM FOR $d=1$

If $d = 1$, the $N\times N$ (even N) fermion matrix is

$$D = D(\mu,m) = \begin{pmatrix}
m & \frac{e^{\mu}}{2} & & & & \frac{e^{-\mu}}{2}\\
-\frac{e^{-\mu}}{2} & m & \frac{e^{\mu}}{2} & & & \\
 & -\frac{e^{-\mu}}{2} & m & \frac{e^{\mu}}{2} & & \\
 & & & \ddots & & \\
 & & & & m & \frac{e^{\mu}}{2}\\
-\frac{e^{\mu}}{2} & & & & -\frac{e^{-\mu}}{2} & m
\end{pmatrix}_{N\times N}.$$

According to a formula of the determinant [59], the determinant of D is

$$\det D = \frac{e^{N\mu}}{2^N} + \frac{e^{-N\mu}}{2^N} + \mathrm{Tr}(T),$$

where the 2×2 transfer matrix T is $T = \begin{pmatrix} m & \frac{1}{4}\\ 1 & 0\end{pmatrix}^N$. Obviously, $\det D > 0$ for any $\mu > 0$ and $m > 0$. Choose n different indices, $1 \le i_1 < \cdots < i_n \le N$, and delete n rows and columns corresponding to these n indices from D to obtain $\tilde D$. We want to prove that the $(N-n)\times(N-n)$ matrix $\tilde D$ satisfies $\det\tilde D > 0$. This holds because the structure of $\tilde D$ is the same as that of D and thus the determinant of $\tilde D$ can be calculated [59], which must be positive. For example, $N = 10$, $n = 2$, $i_1 = 4$, $i_2 = 7$,

$$\tilde D = \left(\begin{array}{ccc|ccc|ccc}
* & * & & & & & & & *\\
* & * & * & & & & & & \\
 & * & * & & & & & & \\
\hline
 & & & * & * & & & & \\
 & & & * & * & & & & \\
\hline
 & & & & & & * & * & \\
 & & & & & & * & * & *\\
* & & & & & & & * & *
\end{array}\right).$$

Since $C(x_1,\ldots,x_{2j})$ can be presented by the determinant of the submatrix of D, which is non-negative, the sign problem is avoided for $d=1$.

APPENDIX C: HEAVY QUARK LIMIT

We introduce notations $X=(x_1,\ldots,x_{d-1})$, $Y=(y_1,\ldots,y_{d-1})$. The matrix element of $\tilde{K}$ in (27) can be written as

$$\tilde{K}_{(t,X),(t,Y)} \equiv (B_t)_{X,Y} = \sum_{\alpha=1,\ldots,d-1} \frac{\eta_{x,\alpha}}{2}((1+iA_\alpha(x))\delta_{x+\hat{\alpha},y} - (1-iA_\alpha(y))\delta_{x,y+\hat{\alpha}}) + m\delta_{x,y}, \qquad t=0,\ldots, \qquad N-1,$$

$$\tilde{K}_{(t,X),(t+1,Y)} = s^+_{x,0}\frac{e^{\mu}}{2}(C_t)_{X,Y}, \qquad (C_t)_{X,Y} \equiv (1+iA_0(x))\delta_{X,Y}, \qquad t=0,\ldots, \qquad N-1,$$

$$\tilde{K}_{(t,X),(t-1,Y)} = -s^-_{x,0}\frac{e^{-\mu}}{2}(C^*_{t-1})_{X,Y}, \qquad t=0,\ldots, \qquad N-1.$$

The matrix $\tilde{K}$ is an $N^d \times N^d$ matrix

$$\tilde{K} = \begin{pmatrix} B_0 & \frac{e^{\mu}}{2}C_0 & & & & & \frac{e^{-\mu}}{2}C^*_{N-1} \\ -\frac{e^{-\mu}}{2}C^*_0 & B_1 & \frac{e^{\mu}}{2}C_1 & & & & \\ & -\frac{e^{-\mu}}{2}C^*_1 & B_2 & \frac{e^{\mu}}{2}C_2 & & & \\ & & & \ddots & & & \\ & & & -\frac{e^{-\mu}}{2}C^*_{N-3} & B_{N-2} & \frac{e^{\mu}}{2}C_{N-2} & \\ -\frac{e^{\mu}}{2}C_{N-1} & & & & -\frac{e^{-\mu}}{2}C^*_{N-2} & B_{N-1} & \end{pmatrix}_{N^d\times N^d}.$$

In the heavy quark limit,

$$m\to\infty, \qquad \mu\to\infty, \qquad \zeta \equiv (2m)^{-1}e^{\mu} \quad \text{fixed}.$$

The matrix $\tilde{K}$ becomes

$$(2m)^{-1}\tilde{K}_{x,y} = \zeta(s^+_{x,0}+iA_0(x))\delta_{x+\hat{0},y} + \delta_{x,y} = \begin{pmatrix} I & \zeta C_0 & & & & 0 \\ 0 & I & \zeta C_1 & & & \\ & 0 & I & \zeta C_2 & & \\ & & & \ddots & & \\ & & & 0 & I & \zeta C_{N-2} \\ -\zeta C_{N-1} & & & & 0 & I \end{pmatrix}_{N^d\times N^d}.$$

The determinant of $\tilde{K}$ satisfies

$$\frac{1}{(2m)^{N^d}}\det\tilde{K} = \det(I+\xi C_{N-1}C_0\cdots C_{N-2}) = \prod_X(1+\xi\mathcal{P}_X),$$

where $\xi=\zeta^N$ and $\mathcal{P}_X=\prod_t(1+A_0(t,X))$ is the Polyakov loop starting and ending at the space point X. The partition function Z in (20) reads

$$
\begin{aligned}
Z &= (2m)^{N^d}\int\prod_{x,\alpha}dA_\alpha(x)\exp\left(-\frac{1}{8U}\sum_{x,\alpha}A_\alpha^2(x)\right)\prod_X(1+\xi\mathcal{P}_X)\\
&= (2m)^{N^d}\left(\frac{1}{2\pi U}\right)^{\frac{(d-1)N^d}{2}}\int\prod_x dA_0(x)\exp\left(-\frac{1}{8U}\sum_x A_0^2(x)\right)\prod_X(1+\xi\mathcal{P}_X)\\
&= (2m)^{N^d}\left(\frac{1}{2\pi U}\right)^{\frac{(d-1)N^d}{2}}\prod_X\int\prod_t dA_0(t,X)\exp\left(-\frac{1}{8U}\sum_t A_0^2(t,X)\right)(1+\xi\mathcal{P}_X)\\
&= (2m)^{N^d}\left(\frac{1}{2\pi U}\right)^{\frac{dN^d}{2}}(1+\xi)^{N^{d-1}},
\end{aligned}
$$

where in the last equality we used

$$
\begin{aligned}
\int\prod_t dA_0(t,X)\exp\left(-\frac{1}{8U}\sum_t A_0^2(t,X)\right)(1+\xi\mathcal{P}_X) &= \left(\frac{1}{2\pi U}\right)^{\frac{N}{2}}+\xi\int\prod_t dA_0(t,X)\exp\left(-\frac{1}{8U}\sum_t A_0^2(t,X)\right)\mathcal{P}_X\\
&= \left(\frac{1}{2\pi U}\right)^{\frac{N}{2}}+\xi\prod_t\int dA_0(t,X)\exp\left(-\frac{1}{8U}A_0^2(t,X)\right)(1+A_0(t,X))\\
&= \left(\frac{1}{2\pi U}\right)^{\frac{N}{2}}+\xi\left(\frac{1}{2\pi U}\right)^{\frac{N}{2}}.
\end{aligned}
$$

In the heavy quantum limit, the chiral condensate and fermion density are

$$
\langle\bar\psi\psi\rangle=\frac{1}{m(1+\xi)},\qquad \langle n\rangle=\frac{1}{1+\frac{1}{\xi}},
$$

respectively, which do not depend on U [5].

APPENDIX D: PHASE-QUENCHED APPROXIMATION

The phase-quenched approximation to (20) is to replace $\det K$ by its module $|\det K|=\sqrt{\det(KK^\dagger)}$,

$$
\begin{aligned}
Z_{\rm pq} &= \int\prod_{x,\alpha}dA_\alpha(x)\exp\left(-\frac{1}{8U}\sum_{x,\alpha}A_\alpha^2(x)\right)|\det K|\\
&= \int\prod_{x,\alpha}dA_\alpha(x)e^{-S_{\rm pq,eff}},
\end{aligned}
\tag{D1}
$$

where the effective action is

$$
S_{\rm pq,eff}=\frac{1}{8U}\sum_{x,\alpha}A_\alpha^2(x)-\frac{1}{2}\ln\det(KK^\dagger).
\tag{D2}
$$

Since

$$
\begin{aligned}
&\frac{\partial}{\partial A_\alpha(x)}\frac{1}{2}\ln\det(KK^\dagger)\\
&\quad=\frac{1}{2}\frac{\partial}{\partial A_\alpha(x)}\mathrm{Tr}\ln(KK^\dagger)\\
&\quad=\frac{1}{2}\mathrm{Tr}\left((KK^\dagger)^{-1}\frac{\partial(KK^\dagger)}{\partial A_\alpha(x)}\right)\\
&\quad=\frac{1}{2}\mathrm{Tr}\left((KK^\dagger)^{-1}\left[\frac{\partial K}{\partial A_\alpha(x)}K^\dagger+K\frac{\partial K^\dagger}{\partial A_\alpha(x)}\right]\right)\\
&\quad=\frac{1}{2}\mathrm{Tr}\left(K^{-1}\frac{\partial K}{\partial A_\alpha(x)}+K^{\dagger-1}\frac{\partial K^\dagger}{\partial A_\alpha(x)}\right)\\
&\quad=\mathrm{Re}\left[\mathrm{Tr}\left(K^{-1}\frac{\partial K}{\partial A_\alpha(x)}\right)\right],
\end{aligned}
$$

the drift force is

$$
-\frac{\partial S_{\rm pq,eff}}{\partial A_\alpha(x)}=-\frac{1}{4U}A_\alpha(x)+\mathrm{Re}\left[\mathrm{Tr}\left(K^{-1}\frac{\partial K}{\partial A_\alpha(x)}\right)\right],
$$

which is just the real part of the complex drift force in (24). This is because the effective action (D2) in the quenched approximation is taken to be the real part of the complex effective action in (22):

$$
\begin{aligned}
e^{-S_{\rm eff}} &= e^{-S_{\rm pq,eff}}e^{i\varphi},\\
e^{i\varphi} &= \frac{\det K}{|\det K|}\iff \mathrm{Re}(\ln\det K)=\frac{1}{2}\ln\det(KK^\dagger).
\end{aligned}
$$

Here the logarithm ln is understood to be the principal value of the logarithm.

The chiral condensate in (25) and fermion density in (26) are replaced by

$$\langle\bar{\psi}\psi\rangle = \frac{1}{N^d}\frac{\partial \ln Z_{\rm pq}}{\partial m} = \frac{1}{N^d}\langle {\rm ReTr}(K^{-1})\rangle_{\rm pq},$$
$$\langle n\rangle = \frac{1}{N^d}\frac{\partial \ln Z_{\rm pq}}{\partial \mu} = \frac{1}{N^d}\left\langle {\rm ReTr}\left(K^{-1}\frac{\partial K}{\partial \mu}\right)\right\rangle_{\rm pq},$$

where the average is taken with respect to the weight of the partition function in (D1). The average phase factor in the phase-quenched theory $\langle e^{i\varphi}\rangle_{\rm pq} = Z/Z_{\rm pq}$ indicates the severeness of the sign problem in the thermodynamic limit.

Since the real function C may be negative, the phase-quenched approximation of (9) is

$$Z_{\rm pq} = \sum_{k=(k_{x,\alpha})} U^j |C(x_1,\ldots,x_{2j})|. \tag{D3}$$

The chiral condensate and fermion density under this phase-quenched approximation are

$$\langle\bar{\psi}\psi\rangle = \frac{1}{N^d}\frac{\partial \ln Z_{\rm pq}}{\partial m} = \frac{1}{N^d}\left\langle\frac{\partial_m C}{C}\right\rangle_{\rm pq},$$
$$\langle n\rangle = \frac{1}{N^d}\frac{\partial \ln Z_{\rm pq}}{\partial \mu} = \frac{1}{N^d}\left\langle\frac{\partial_\mu C}{C}\right\rangle_{\rm pq},$$

respectively. The average phase factor is

$$\langle e^{i\varphi}\rangle_{\rm pq} = \left\langle\frac{C}{|C|}\right\rangle_{\rm pq} = \frac{\sum_{k=(k_{x,\alpha})} U^j C(x_1,\ldots,x_{2j})}{\sum_{k=(k_{x,\alpha})} U^j |C(x_1,\ldots,x_{2j})|}.$$

Here the average $\langle\rangle_{\rm pq}$ is taken with respect to the partition function $Z_{\rm pq}$ in (D3).

[1] G. Fredrickson, *The Equilibrium Theory of Inhomogeneous Polymers* (Oxford University Press, New York, 2006).
[2] D. Li, K. Liang, and T. Gruhn, Macromol. Symp. **346**, 22 (2014).
[3] G. Aarts, F. A. James, E. Seiler, and I.-O. Stamatescu, Phys. Lett. B **687**, 154 (2010).
[4] G. Aarts, Phys. Rev. Lett. **102**, 131601 (2009).
[5] J. M. Pawlowski and C. Zielinski, Phys. Rev. D **87**, 094509 (2013).
[6] J. Flower, S. W. Otto, and S. Callahan, Phys. Rev. D **34**, 598 (1986).
[7] D. Sexty, Phys. Lett. B **729**, 108 (2014).
[8] G. Aarts and I.-O. Stamatescu, J. High Energy Phys. 09 (2008) 018.
[9] G. Aarts, F. A. James, J. M. Pawlowski, E. Seiler, D. Sexty, and I.-O. Stamatescu, J. High Energy Phys. 03 (2013) 073.
[10] G. Aarts and F. A. James, J. High Energy Phys. 01 (2012) 118.
[11] G. Aarts, L. Bongiovanni, E. Seiler, D. Sexty, and I.-O. Stamatescu, Eur. Phys. J. A **49**, 89 (2013).
[12] J. Berges and I.-O. Stamatescu, Phys. Rev. Lett. **95**, 202003 (2005).
[13] J. Berges, S. Borsanyi, D. Sexty, and I.-O. Stamatescu, Phys. Rev. D **75**, 045007 (2007).
[14] J. Berges and D. Sexty, Nucl. Phys. **B799**, 306 (2008).
[15] G. Aarts and F. A. James, J. High Energy Phys. 08 (2010) 020.
[16] J. M. Pawlowski and C. Zielinski, Phys. Rev. D **87**, 094503 (2013).
[17] H. W. Hamber and H. Ren, Phys. Lett. **159B**, 330 (1985).
[18] J. Flower, S. W. Otto, and S. Callahan, Phys. Rev. D **34**, 598 (1986).
[19] E.-M. Ilgenfritz, Phys. Lett. B **181**, 327 (1986).
[20] G. Aarts, F. A. James, E. Seiler, and I.-O. Stamatescu, Eur. Phys. J. C **71**, 1756 (2011).
[21] G. Guralnik and C. Pehlevan, Nucl. Phys. **B811**, 519 (2009).
[22] G. Guralnik and C. Pehlevan, Nucl. Phys. **B822**, 349 (2009).
[23] G. Guralnik and Z. Guralnik, Ann. Phys. (Amsterdam) **325**, 2486 (2010).
[24] G. Aarts, E. Seiler, and I.-O. Stamatescu, Phys. Rev. D **81**, 054508 (2010).
[25] G. Aarts, P. Giudice, and E. Seiler, Ann. Phys. (Amsterdam) **337**, 238 (2013).
[26] A. Mollgaard and K. Splittorff, Phys. Rev. D **88**, 116007 (2013).
[27] G. Aarts, L. Bongiovanni, E. Seiler, and D. Sexty, J. High Energy Phys. 10 (2014) 159.
[28] J. Nishimura and S. Shimasaki, Phys. Rev. D **92**, 011501 (2015).
[29] S. Tsutsui and T. M. Doi, Phys. Rev. D **94**, 074009 (2016).
[30] T. Hayata, Y. Hidaka, and Y. Tanizaki, Nucl. Phys. **B911**, 94 (2016).
[31] C. Gattringer and T. Kloiber, Nucl. Phys. **B869**, 56 (2013).
[32] Y. D. Mercado and C. Gattringer, Nucl. Phys. **B862**, 737 (2012).
[33] Y. D. Mercado, C. Gattringer, and A. Schmidt, Comput. Phys. Commun. **184**, 1535 (2013).
[34] C. Gattringer, T. Kloiber, and V. Sazonov, Nucl. Phys. **B897**, 732 (2015).
[35] F. Bruckmann, C. Gattringer, T. Kloiber, and T. Sulejmanpasic, *Proc. Sci.*, LATTICE2015 (2016) 210 [arXiv:1512.05482].
[36] F. Bruckmann, C. Gattringer, T. Kloiber, and T. Sulejmanpasic, Phys. Lett. B **749**, 495 (2015).

[37] U. Wolff, Nucl. Phys. **B824**, 254 (2010); **B834**, 395(E) (2010).
[38] U. Wolff, Nucl. Phys. **B832**, 520 (2010).
[39] S. Chandrasekharan, Eur. Phys. J. A **49**, 1 (2013).
[40] S. Chandrasekharan and A. Li, *Proc. Sci.*, LATTICE2011 (2011) 058 [arXiv:1111.5276].
[41] S. Chandrasekharan and A. Li, *Proc. Sci.*, LATTICE2012 (2012) 225 [arXiv:1202.6572].
[42] S. Chandrasekharan, Phys. Rev. D **86**, 021701 (2012).
[43] R. Oeckl and H. Pfeiffer, Nucl. Phys. **B598**, 400 (2001).
[44] J. W. Cherrington, D. Christensen, and I. Khavkine, Phys. Rev. D **76**, 094503 (2007).
[45] J. W. Cherrington, Nucl. Phys. **B794**, 195 (2008).
[46] H. Pfeiffer, J. Math. Phys. (N.Y.) **44**, 2891 (2003).
[47] Z.-X. Li, Y.-F. Jiang, and H. Yao, Phys. Rev. B **91**, 241117 (2015).
[48] Z.-X. Li, Y.-F. Jiang, and H. Yao, arXiv:1601.05780.
[49] Z. C. Wei, C. Wu, Y. Li, S. Zhang, and T. Xiang, Phys. Rev. Lett. **116**, 250601 (2016).
[50] D. Banerjee, F.-J. Jiang, M. Kon, and U.-J. Wiese, Phys. Rev. B **90**, 241104 (2014).
[51] G. Cohen, E. Gull, D. R. Reichman, and A. J. Millis, Phys. Rev. Lett. **115**, 266802 (2015).
[52] E. F. Huffman and S. Chandrasekharan, Phys. Rev. B **89**, 111101 (2014).
[53] E. F. Huffman and S. Chandrasekharan, Phys. Rev. E **94**, 043311 (2016).
[54] D. Spielmann, Aspects of confinement in QCD from lattice simulations, Ph.D. thesis, Ruprecht-Karls-Universität Heidelberg, 2010.
[55] H. Gies and L. Janssen, Phys. Rev. D **82**, 085018 (2010).
[56] D. Li, arXiv:1605.04623.
[57] H. J. Rothe, *Lattice Gauge Theory: An Introduction*, World Scientific Lecture Notes in Physics Vol. 74 (World Scientific Publishing Co. Pte. Ltd., Singapore, 2005).
[58] U. Wolff, Comput. Phys. Commun. **156**, 143 (2004).
[59] L. G. Molinari, Linear Algebra Appl. **429**, 2221 (2008).